

THE X-RAY CRYSTAL STRUCTURE OF THROMBIN IN COMPLEX WITH N α -2-NAPHTHYLSULFONYL-L-3- AMIDINO-PHENYLALANYL-4-METHYLPYRIDIDE: THE BENEFICIAL EFFECT OF FILLING OUT AN EMPTY CAVITY

ANDREAS BERGNER¹, MARGIT BAUER¹, HANS BRANDSTETTER¹,
JÖRG STÜRZEBECKER² and WOLFRAM BODE^{1*}

¹*Max-Planck-Institut für Biochemie, D-82152 Martinsried b.
München, Germany*

²*Klinikum der Friedrich-Schiller-Universität Jena,
Zentrum für Vaskuläre Biologie und Medizin,
D-99089 Erfurt, Germany*

(Received 1 November 1994)

The 2.5 Å structure of bovine ϵ -thrombin in complex with N α -2-naphthyl-sulfonyl-L-3-amidinophenylalanyl-4-methylpyridide (L-NAPAMP) was solved and crystallographically refined to an *R*-value of 0.19. The L-NAPAMP moiety is completely and unambiguously defined in the electron density. NAPAMP binds almost identical to the related 4-methyl deficient 3-amidino-phenylalanyl derivative TAPAP. The overall binding geometry appears dominated by the fixation of the 3-amidinophenyl ring in thrombin's S1-pocket and the hydrogen bonds to Gly 216, irrespective of the presence or absence of a substituent in the 4-position of the piperidine ring. The additional 4-methyl group gives rise to a 17-fold better binding. The more complete spatial occupancy of the hydrophobic S2-cavity therefore accounts for a decrease in free energy of binding of 15 kcal/mol, a value comparable with that anticipated for filling up a stable empty cavity of similar size by a methyl group.

KEY WORDS: Thrombin, antithrombotics, inhibitors, X-ray crystal structure, inhibitor complex

INTRODUCTION

Inhibitors acting directly on thrombin exhibit a number of advantages over the currently used therapeutical anticoagulants (heparin, warfarin), which meet some but not all of the criteria for an ideal antithrombotic drug.¹ From this point of view, both the naturally occurring thrombin inhibitors hirudin² and the synthetic peptide hirulog³ are quite promising anticoagulants. Due to their peptidic nature, however, these agents can only be administered by the parenteral route. In contrast to large peptides and recombinant proteins, synthetic low-molecular weight inhibitors are potentially

* Correspondence

able to be absorbed following oral application. Thus, a synthetic orally applicable inhibitor which is selective towards thrombin and exhibits a sufficient half-life in the circulation is potentially an ideal anticoagulant. Partial absorption following oral administration has been shown for antithrombotically active peptide aldehydes,⁴ boronic acid derivatives⁵ and benzamidine-derived inhibitors.⁶ The absorption rate of these compounds is still not high enough, and there is room for improvement in their pharmacokinetic properties.

The benzamidine moiety, which mimics the guanidinoalkyl side chain of arginine, is one of the key structures for the development of thrombin inhibitors. The most potent thrombin inhibitor of the benzamidine type is *N* α -2-naphthylsulfonyl-glycyl-DL-4-amidinophenylalanyl-piperidide (NAPAP, see Figure 1). However, NAPAP and related benzamidine-inhibitors do not fulfill the pharmacological requirement for an ideal anticoagulant.^{6,7} The X-ray crystal structure of a NAPAP-thrombin complex^{8,9} showed that the structural changes required to improve the pharmacokinetic behaviour would result in a loss in inhibitory potency.^{10,11} Meanwhile we have found a new benzamidine based lead structure, namely *N* α -4(toluenesulfonyl)-DL-3-amidinophenylalanyl-piperidide (TAPAP, see Figure 1).¹² Trypsin- and thrombin-TAPAP complex structures indicated free intermolecular space, both at the toluene ring as well as in the piperidine moiety^{8,13} available for derivatization.

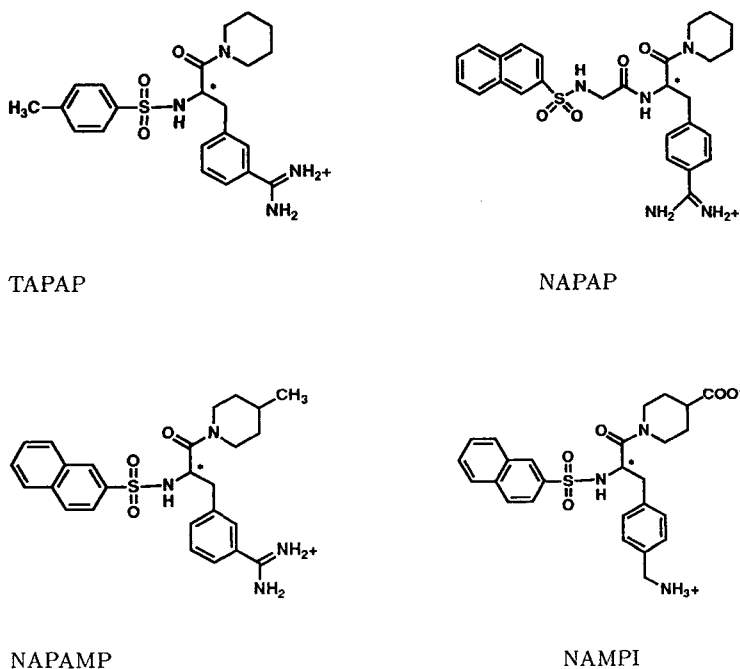


FIGURE 1 Chemical formulas of TAPAP, NAPAP, NAPAMP and NAMPI. The asterisk indicates the chiral center.

TABLE 1
Inhibition constants (K_i , $\mu\text{mol/l}$) for bovine thrombin and bovine trypsin

Inhibitor	Enantiomer	Thrombin	Trypsin
NAPAMP	D,L	0.0062	0.14
NAPAMP	L	0.0025	0.042
NAPAMP	D	0.96	24.3
TAPAP	D,L	0.34	1.3
NAPAP	D,L	0.006	0.69
NAPAP	L	1.4	25.5
NAPAP	D	0.0021	0.21

A large number of new derivatives of 3-amidinophenylalanine have been synthesized¹⁴. Of this series, the racemate of $N\alpha$ -naphthylsulfonyl-3-amidinophenylalanyl-4-methylpiperidide NAPAMP (see Figure 3) exerts high antithrombin activity equal to that of DL-NAPAP (K_i 6.2 and 6.0 nmol/l, respectively (see Table 1)).⁷ Although substituents which normally improve absorption behaviour upon oral application and reduce rapid elimination from the circulation could be introduced into the molecule without loss of activity, only low absorption rates were determined.⁶ Further derivatizations are therefore necessary to improve these pharmacokinetic properties. The present crystallographic study is aimed at directing such synthetic modifications.

MATERIALS AND METHODS

Bovine α -thrombin was prepared from ox blood, purified and incubated with pancreatic elastase in order to generate ε -thrombin.⁸ Octahedral crystals of dimensions up to 0.8 mm were grown using the vapour diffusion method as described elsewhere.⁸ The sample drops contained about 10 mg/ml of bovine ε -thrombin and 1.0 mg/ml of D- or L-NAPAMP, respectively. The crystals belong to the tetragonal space group $P4_22_12$ and have cell constants of about $a = b = 88.9$ and $c = 103.3$ Å. The crystals contain one molecule per asymmetric unit and diffract to almost 2.4 Å. The synthesis of NAPAMP has been described elsewhere.¹⁴

X-ray data were collected at 7°C on a MAR imaging plate system, using a crystal detector to distance of 130 mm. Only reflections with $I > 2\sigma$ were considered as significant. The reflection data (Table 2) were evaluated using the indexing and integrating routines of the MOSFLM package¹⁵ and loaded and scaled with the PROTEIN program.¹⁶ Initial rigid body refinement was done with XPLOR¹⁷ using the refined model of bovine ε -thrombin.⁸ Subsequently this model was subjected to the restrained least squares refinement implemented in XPLOR, using the force-field

TABLE 2
Reflection data for the bovine ϵ -thrombin crystals in complex with D- and L-NAPAMP

	D-NAPAMP	L-NAPAMP
Limiting resolution Å	2.45	2.6
Number of significant measurements	71033	61618
Number of independent reflections	14633	11994
R _{merge}	0.062	0.126
completeness	93.2%	91.5%
cell constants (Å)		
a = b	88.94	88.89
c	103.34	103.45

parameter derived from the chemical structures stored in the Cambridge Structure Data Bank.¹⁸ When the R-values decreased to 0.274, the NAPAMP model generated from TAPAP¹³ was fitted to the electron density in the thrombin binding site and was co-refined with the thrombin molecule using parameters as described elsewhere.⁸ In the final stage, a constrained B-factor refinement was also performed, which decreased the R-value to 0.190. The final model parameters are given in Table 3.

TABLE 3
Final model and refinement parameters

	D-NAPAMP	L-NAPAMP
Number of total non-hydrogen protein atoms	2609	2609
hydrogen protein atoms	2454	2454
Number of non-hydrogen inhibitor atoms	39	39
Number of solvent molecules	225	225
r.m.s. standard dev. from target values		
Bond lengths (Å)	0.016	0.009
Bond angles (deg.)	2.008	1.623
Number of reflections		
used for refinements	13695	11765
Resolution range Å	8.0 to 2.5	8.0 to 2.6
R-value ⁱ	0.198	0.190

$$\sum (|F_{\text{obs}}| - |F_{\text{calc}}|) / \sum |F_{\text{obs}}|$$

RESULTS

The thrombin moiety

The thrombin moiety[†] of the bovine thrombin complex investigated in this study is nearly identical in structure to three other bovine thrombin complexes crystallizing in the same tetragonal space group as previously described.⁸ The rms deviation of all defined α -carbon atoms between these different complexes is around 0.42 Å, close to that expected for a comparison of two structures with estimated mean positional errors of 0.35 Å obtained from Luzzati plots. Interestingly, the thrombin residues forming the inhibitor binding site (such as the 60 loop shaping the S2 cavity^{19,20}), exhibit slightly smaller deviations.

The L-NAPAMP-thrombin structure

Figure 2 displays a section of the final electron density of the L-NAPAMP-thrombin complex around the active site, superimposed with the equivalent part of the refined model. The L-NAPAMP molecule is bound to the “fibrinopeptide side”,^{19,21} i.e. to the “west” of the active site of thrombin in Figures 3–5. It is well defined by electron density, and in particular confirms the anticipated L-configuration at the central carbon atom. Its main chain juxtaposes thrombin segment Ser 214–Gly 216 in an antiparallel, slightly twisted manner forming two hydrogen bonds of lengths 2.7 and 2.9 Å between the amino nitrogen and the carbonyl oxygen of the central 3-amidinophenylalanine residue and Gly 216 O and N of thrombin, respectively. The amidinophenyl moiety is arranged in a similar manner to that of the closely related TAPAP (see Figure 4), i.e. it is sandwiched between thrombin segments Ala 190–Glu 192 and Trp 215–Gly 216, which together with the interconnecting disulfide bridge 191–220 form the “base” and the “ceiling” of the thrombin specificity pocket, respectively. Due to the 3-position of the amidino group, its two nitrogens can juxtapose the two carboxylate oxygens of Asp 189 situated at the bottom of the specificity pocket, under formation of favourable 3.1 Å hydrogen bonds of twin N-twin O contact type.⁸

The β -naphthyl group of L-NAPAMP is almost perpendicular to the indol moiety of Trp 215 and nestles into the characteristic aryl binding site^{10,19} of thrombin (Figure 3). It might be noteworthy that the same β -naphthyl group in the closely related N α -2-naphthylsulfonyl-L-3-aminomethylphenylalanyl-isonipecotic acid (NAMPI) thrombin structure⁶ is rotated 180° around S-C, pointing away from Trp 215. In the NAPAMP-thrombin structure, both sulfonyl oxygens are directed towards Gly 219 N and away from the thrombin surface, respectively. The 4-methylpiperidine ring of L-NAPAMP is clearly confined to one distinct chair conformation and is squeezed between the naphthyl moiety and the His 57 imidazole side chain of thrombin, i.e. in an identical manner to the piperidine ring of TAPAP (see Figure 4). The 4-methyl group is arranged in an equatorial position and fills the space in the cavity formed by

[†]The chymotrypsinogen nomenclature of thrombin as introduced by Bode *et al.*^{19,20} is used throughout this paper.

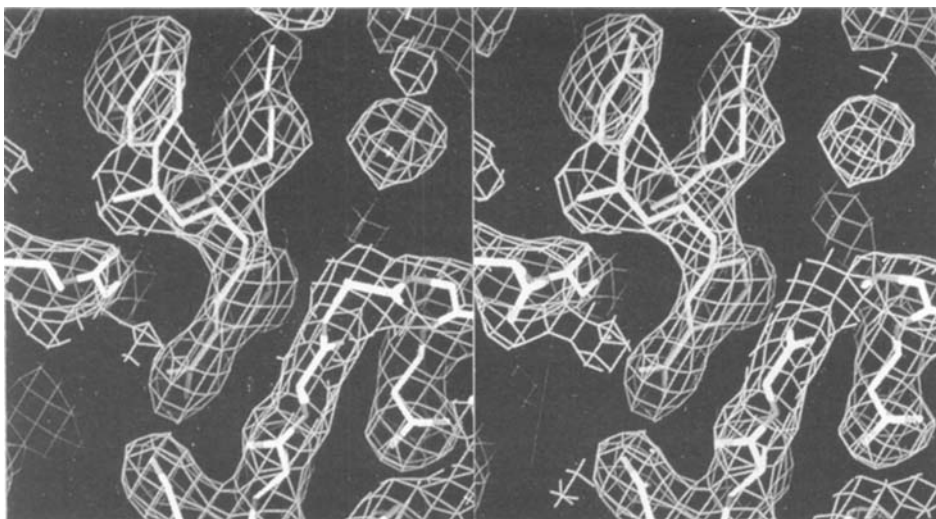


FIGURE 2 Stereo plot of the active site region of the complex formed between L-NAPAMP (yellow-green) and bovine thrombin (white-blue-red for carbons, nitrogens and oxygens) superimposed with the final $2F_{\text{obs}} - F_{\text{calc}}$ electron density. Contouring at 1.0σ . Made with program O²⁵.

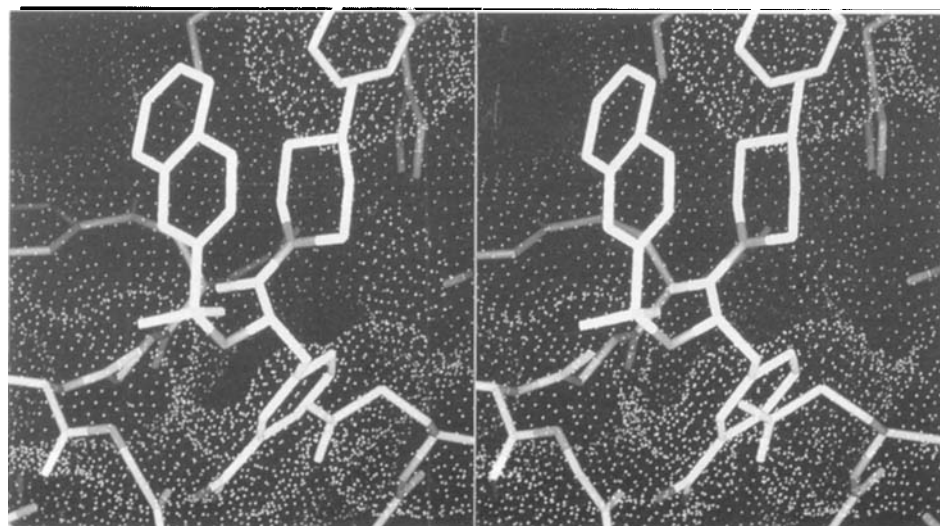


FIGURE 3 Stereo plot of the active site region of the complex formed between L-NAPAMP and bovine thrombin (white-blue-red), superimposed with a Connolly dot surface (blue). The view is the “standard view”^{19,20} also used in Figures 3 to 5, i.e. from outside onto the active site, with a peptide substrate binding along the horizontal active site cleft from left to right. Trp 60D of the 60 loop (top, front) is partially visible, and the active site residues Ser 195 and His 57 (right) are only represented by their OG atom and the imidazole ring, respectively. Figures 3 to 5 are prepared using program Main.²⁶



FIGURE 4 Stereo plot of the active site region of the complex formed between NAPAMP (yellow) and bovine thrombin (green-blue-red), superimposed with TAPAP (pink) and the Connolly dot surface of thrombin.

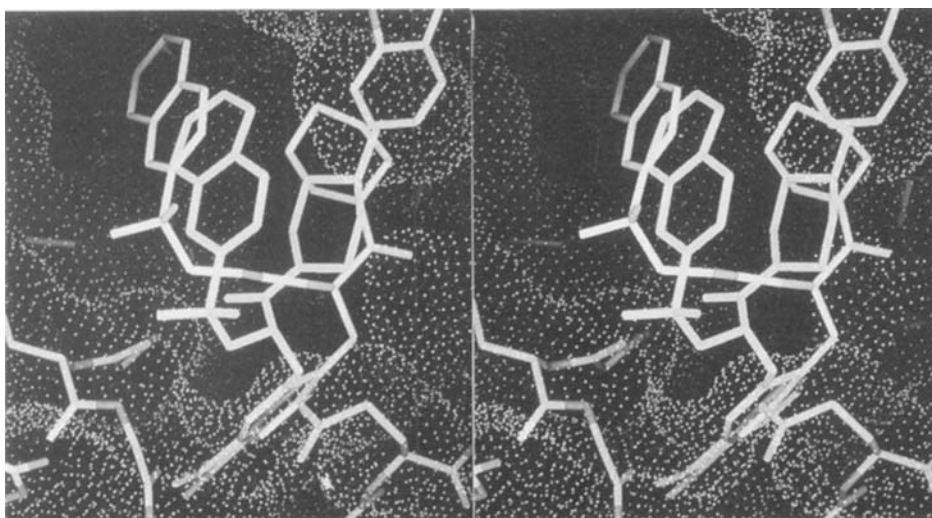


FIGURE 5 Stereo plot of the active site region of the complex formed between NAPAMP (yellow) and bovine thrombin (green-blue-red), superimposed with NAPAP (pink) and the Connolly dot surface of thrombin.

the thrombin side chains of His 57, Tyr 60 A and Trp 60D and by the piperidine moiety of L-NAPAMP to a large extent. An axial 4-methyl group site would lead to collision with the His 57 imidazole side chain.

The D-NAPAMP-thrombin structure

We tried to determine also the structure of the thrombin complex with D-NAPAMP, following the same procedures as with L-NAPAMP (see Tables 2 and 3). The initial and the final density around the bound inhibitor was very similar to that of L-NAPAMP-thrombin, but was not compatible with a bound D-stereoisomer. We therefore conclude that the minor amounts of L-form still present in the purified D-sample are preferentially bound in the crystal.

DISCUSSION

Structural analysis of both NAPAMP-thrombin complexes revealed a very similar mode of binding of L-NAPAMP to that of the TAPAP lead structure, in spite of the substitution of the toluene by the naphthyl group and enlargement of the piperidine moiety by a methyl group. The position and orientation of the inhibitor “main chain” would appear to be largely determined by fixation of the 3-amidinophenyl group in the S1 pocket and by the antiparallel binding along Ser 214 to Gly 216, which together impair any larger shift or rotation of the inhibitor. Filling out of the empty hole observed in the S2 cavity of the TAPAP-thrombin structure by the methyl group is in full agreement with earlier suggestions obtained from our modelling experiments.^{8,13} The better packing of the β -naphthylsulfonyl and of the 4-methylpiperidine group compared with the toluenesulfonyl and the unsubstituted piperidine, respectively, is paralleled by a considerable 55-fold increase in binding (compare Table 1), corresponding to a decrease in (negative) free energy of binding of 2.4 kcal/mol. Neglecting differences in desolvation energy and motional freedom, this free energy change can be roughly decomposed into fractions accounting for the better fit of the naphthyl moiety (-0.9 kcal/mol) and the 4-methyl group (-1.5 kcal/mol), respectively. This latter value is in the range generally observed for putting a methyl group into a stable empty cavity of appropriate size.^{22,23} Comparison with NAPAP-thrombin (see Figure 5) and NAMPI-thrombin,⁶ where the S2 pocket is more fully occupied by a piperidine ring and a 4-carboxylate group, respectively, indicates, that the hole left by the nonsubstituted piperidine ring in the TAPAP analogues surpasses even the size of a methyl group. Studies with L-NAPAMP analogues indeed show that 4-piperidine substituents up to the size of a methoxycarbonyl group can be accommodated without much loss in affinity.¹⁴

From the crystal structure (Figure 4) we conclude that the β -naphthyl moiety of NAPAMP is better suited to fill the hydrophobic furrow of the aryl binding site than the smaller toluene group of TAPAP, in agreement with the observed decrease in free energy of binding of 0.9 kcal/mol. Due to the “lower” position of the “main chain” of NAPAMP relative to Ser 214–Gly 216, the naphthyl group of NAPAMP cannot fill the aryl binding site to a similar extent to that of NAPAP, however (see

Figure 5). This presumably results in slightly weaker interactions, which might explain the different naphthyl orientation in the related NAMPI-thrombin structure.⁶ These weaker interactions in the aryl site are presumably compensated by closer contacts at the base, as D-NAPAP and L-NAPAMP have identical K_i -values (see Table 1). In the thrombin bound states of the benzamidine derived inhibitors mentioned here, both terminal (naphthyl and piperidine) groups are folded together into a compact entity. Presumably, this conformation is close to the preferred conformation in solution, resulting in tight binding due to entropically favourable conditions. Such a preformation of the binding geometry in the isolated (solution) state contributes considerably to tight binding of high affinity inhibitors (see for PPACK²⁴).

As previously established,^{8,11} another important factor in complex stabilisation is the exploitation of full hydrogen bonding capacity to Gly 216, provided in L-NAPAMP by the amido groups flanking the central 3-amidinophenylalanyl moiety. Model studies with D-NAPAMP show that the D-stereoisomer might be bound to the same subsites of thrombin, with all three “side chains” involved in contact similar to those utilized by the L-enantiomer. Such a binding geometry of the D-enantiomer would not be compatible with simultaneous formation of one or both hydrogen bonds to Gly 216, however. The 400-fold (or higher, see below) increase in K_i when going from the D- to the L-enantiomer seems primarily be related to the incapability to form these hydrogen bonds under simultaneous shielding of both Gly 216 polar groups from contacts with bulk water. We conclude that the separation of the D- from the L-form during synthesis was not sufficient to exclude trace amounts of the latter, which are then enriched in the thrombin complexes during crystallization due to the high excess of the inhibitor over thrombin and the much lower K_i of the L-form. Therefore, the K_i -value for D-NAPAMP as given in Table 1 should be considered to represent a lower boundary only.

Our studies show that the 3-amidinophenylalanine derived inhibitors bind to thrombin in a relatively invariable manner independent of their substituents, i.e. without much rearrangement. This validates the use of simple modelling experiments assuming relatively rigidly fixed geometries to suggest appropriate inhibitor modifications in this family of inhibitors.

Acknowledgements

We would like to thank Prof. Robert Huber for his constant support and interest in this work, Dr. M.T. Stubbs for reviewing this manuscript, and the financial support of the SFB 207.

References

1. Sixma, J.J. and de Groot, P.G. (1992) *Thromb. Res.*, **68**, 507–512.
2. Markwardt, F. (1994) *Thromb. Res.*, **74**, 1–23.
3. Maraganore, J.M., Bourdon, P., Jablonski, J., Ramachandran, K.L. and Fenton II, J.W. (1990) *Biochemistry*, **29**, 7095–7101.
4. Bajusz, S., Szell, E., Bagdy, D., Barabas, E., Horvath, G., Dioszegi, M., Fittler, Z., Szabo, G., Juhasz, A., Tomori, E. and Szilagyi, G. (1990) *J. Med. Chem.*, **33**, 1729–1735.
5. Hussain, M.A., Knabb, R., Aungst, B.J. and Kettner, C. (1991) *Peptides*, **12**, 1153–1154.

6. Stürzebecher, J., Prasa, D., Bretschneider, E., Bode, W., Bauer, M., Brandstetter, H., Wikström, P. and Vieweg, H. (1993) in: *DIC-Pathogenesis, Diagnosis and Therapy of Disseminated Intravascular Fibrin Formation*. (G. Müller-Berghaus, K. Madlener, M. Blombäck and J.W. ten Cate, Eds.) pp. 183–190. Amsterdam, London, New York, Tokyo: Excerpta Medica.
7. Stürzebecher, J., Markwardt, F., Voigt, B., Wagner, G. and Walsmann, P. (1983) *Thromb. Res.*, **29**, 635–642.
8. Brandstetter, H., Turk, D., Hoeffken, H.W., Grosse, D., Stürzebecher, J., Martin, P.D., Edwards, B.F.P. and Bode, W. (1992) *J. Mol. Biol.*, **226**, 1085–1099.
9. Banner, D.W. and Hadvary, P. (1991) *J. Biol. Chem.*, **266**, 20085–20093.
10. Bode, W., Turk, D. and Stürzebecher, J. (1990) *Eur. J. Biochem.*, **193**, 175–182.
11. Bauer, M., Brandstetter, H., Turk, D., Stürzebecher, J. and Bode, W. (1993) *Semin. Thromb. Hemost.*, **19**, 352–360.
12. Markwardt, F., Wagner, G., Stürzebecher, J. and Walsmann, P. (1980) *Thromb. Res.*, **17**, 425–431.
13. Turk, D., Stürzebecher, J. and Boyle, W. (1991) *FEBS Lett.*, **287**, 133–138.
14. Stürzebecher, J., Prasa, D., Wikström, P. and Vieweg, H. (1994) *J. Enz. Inhibit.*, this issue.
15. Leslie, A.G.W. (1991) in: *CCF4 and ESF-EACMB Newsletters on Protein Crystallography*. SERC Laboratory, Darresbury.
16. Steigemann, W. (1974) *PhD Thesis Technische Universität München*.
17. Brünger A.T., Karplus, M. and Petsko, G.A. (1989) *Acta Cryst.*, **A45**, 50–61.
18. Engh, R. and Huber, R. (1991) *Acta Cryst.*, **A47**, 392–400.
19. Bode, W., Turk, D. and Karshikov, A. (1992) *Protein Sci.*, **1**, 426–471.
20. Stubbs, M.T. and Bode, W. (1993) *Thromb. Res.*, **69**, 1–58.
21. Bode, W., Mayr, I., Baumann, U., Huber, R., Stone, S.R. and Hofsteenge, J. (1989) *EMBO J.*, **8**, 3467–3475.
22. Bode, W. (1979) *J. Mol. Biol.*, **127**, 357–374.
23. Jackson, S.E., Moracci, M., elMasry, N., Johnson, C.M. and Fersht, A.T. (1993) *Biochemistry*, **32**, 11259–11269.
24. Lim, M.S.L., Johnson, E.R. and Kettner, C.A. (1993) *J. Med. Chem.*, **36**, 1831.
25. Jones, T.A., Zou, J.Y., Cowen, S.W. and Kjeldgard, M. (1991) *Acta Cryst.*, **A47**, 110–119.
26. Turk, D. (1992) *PhD Thesis Technische Universität München*.